JOURNAL OF GUIDANCE, CONTROL, AND DYNAMICS
Vol. , No. ,

Space Debris Attitude Control During Contactless Transportation in Planar Case

Vladimir S. Aslanov* and Alexander S. Ledkov†
Samara National Research University, 443086, Samara, Russia

1 https://doi.org/10.2514/1.G004686

The use of ion flow for the implementation of contactless force action transmission from an active spacecraft to a passive object is a promising technology for the creation of active large space debris removal systems. Keeping a certain orientation of large space debris with respect to the oncoming ion stream in the process of its removal from the orbit can significantly reduce the time for this transport operation. The aim of the work is to develop a control law that stabilizes the space debris in a certain position. A cylindrical spent rocket stage is considered as the space debris. The planar motion of a mechanical system consisting of the active spacecraft and the space debris is considered. The two ways to control the ion flux are considered and compared with each other: by changing the thrust of the ion engine and by turning the ion flow direction. Lyapunov's theorems on stability and asymptotic stability in the first approximation and Bellman method are used to build the control laws. The results of numerical simulation prove that controlling the ion flow direction is a more efficient way of stabilizing attitude motion in terms of minimizing the time spent.

Nomenclature

b_i = Fourier coefficients of ion beam torque expansion, $\mathrm{N \cdot m}$
c_i = coefficients of the ion beam torque decomposition, $\mathrm{N \cdot m}$
d = distance between the spacecraft and the space debris center of mass, m
F_x, F_y = projections of the ion beam force on the axes of the body coordinate system, N
I_x = longitudinal moment of inertia of the space debris, $\mathrm{kg \cdot m^2}$
I_y, I_z = transversal moments of inertia of the space debris, $\mathrm{kg \cdot m^2}$
k = constant control parameter
L = Lagrange function, J
$\boldsymbol{L}^{\max}$ = maximum ion beam torque vector that the ion engine can provide, $\mathrm{N \cdot m}$
L_z = ion beam torque, $\mathrm{N \cdot m}$
m_A, m_B = mass, kg
m_0 = ion mass, kg
n_0 = plasma density at the beginning of the far region, $\mathrm{m^{-3}}$
P_x, P_x = spacecraft control engine's thrust force projections, N
Q_j = nonpotential generalized forces
q_j = component of the generalized coordinates vector
R_0 = radius of the beam at the beginning of the far region, m
r = distance between the center of the Earth and the spacecraft, m
S_j = area of jth triangle, m^2
T = kinetic energy, J
U = potential energy, J
u = dimensionless control parameter
V = Lyapunov function
V_A, V_B = velocity, m/s
V_0 = axial component of the ion flus velocity, m/s
$V_0^{\max}$ = maximum axial component of the ion flux that the ion engine can provide, m/s
v = true anomaly angle, rad
w = dimensionless control function
x = coordinate of the center of mass, m
y = coordinate of the center of mass, m
α = angle of deviation of the line connecting the spacecraft and the center of mass of the space debris from the local horizon of the spacecraft, rad
α_0 = divergence angle of the ion beam, rad
β = ion flow axis deflection angle, rad
γ = deflection angle of the longitudinal axis of space debris from its local vertical, rad
ε = small value
θ = space debris deflection angle, rad
μ = gravitational constant of the Earth, $\mathrm{m^3 \cdot s^{-2}}$
τ = dimensionless independent variable
ω = spacecraft orbital angular velocity, rad/s

Subscripts

A = spacecraft
B = space debris center of mass

I. Introduction

SPACE debris mitigation is one of the most important challenges of modern astronautics. The risk of mutual collisions of nonfunctioning satellites and spent rocket stages in orbit makes it an urgent task to search for means of active space debris removal. A detailed overview of existing active space debris removal methods is given in [1–3]. Contactless methods of cleaning space debris are of great interest. The main advantage of contactless transportation of a passive space object is the absence of the need to dock with it. Several possible methods of contactless influence on the passive object are discussed in the scientific literature: using space-based lasers [4–6], using an electrostatic field [7–9], and using an ion flux created by the ion engine of an active spacecraft [10–13]. Contactless transportation due to electrostatic forces requires the placement of sophisticated
equipment on the active spacecraft for the transfer of charge on the 2
passive object. This method does not work well in low Earth orbit because the plasma is too cold and dense. The ion beam transportation could work at all altitudes, but it is requiring more fuel because the second engine must be used to compensate the thrust force created by the ion flow, which blows the passive object. The active spacecraft should be at a distance of about 10 m from space debris for successful transportation. Because the shape of the flow is close to the cone, an increase in this distance leads to an increase in the fraction of ions that are wasted so far as they do not collide with the surface of the object.

Received 2 July 2019; revision received 7 October 2019; accepted for publication 8 October 2019; published online XX epubMonth XXXX.

*Head of Department, Professor, Theoretical Mechanics Department, 34, Moscovskoe Shosse.

†Associate Professor, Theoretical Mechanics Department, 34, Moscovskoe Shosse.

In this study, we will focus on the ion beam transportation method. It is assumed that an active spacecraft approaches space debris and directs an ion beam at it. Ions colliding with the surface of space debris exert a force on it. To keep the active spacecraft near the space debris, the spacecraft includes a second ion engine, which is directed opposite to the first one and neutralizes its force effect. This scheme of contactless transportation is called "ion-beam shepherd." An analysis of the literature shows that the question of determining the forces and moments transmitted by the ion flow to a blown rigid body is studied in detail [14–16]. Estimates of the time it takes for space debris to be removed from the spacecraft are given in various papers [10,11]. Space debris with a mass of several tons can be removed from a 1000 km orbit for several months. Simulation of the motion of the ion-flowed spent rocket stage around its center of mass, taking into account gravitational, ionic, and aerodynamic moments, is carried out in [17]. The control laws of an active spacecraft are proposed in studies [18–20] without taking into account the rotation of space debris with respect to its center of mass. In [11], it was shown that the attitude motion of space debris significantly affects the time required to change orbits. In particular, the upper stage of the Cosmos 3M rocket stage descent from a height of 500 km to 100 km in the case of free oscillations for about 180 days. In the case of the rocket stage stabilization perpendicular to the ion flow this time decreases to 120 days. The spatial orientation of the body relative to the oncoming ion flux, which ensures the fastest removal of the body from the orbit and depends on the mass-geometric parameters of the body, can be found. Thus, the task of stabilizing space debris in some position arises. The task of detumbling and stabilization of a passive object also arises when the docking or capturing of the object with an active spacecraft is required, for example, for its service maintenance or tethered towing.

The aim of the work is to develop a control law that ensures the stabilization of a passive object in a certain position. The stabilization process can be divided into two stages. The first stage is the reduction of the angular velocity of the passive object rotation, and its translation into oscillation mode. The second stage is a decrease in the oscillation amplitude of the passive object. The analysis of the phase portrait performed in [11] shows that a decrease in the angular velocity can be performed by deflecting the axis of the ion beam in the direction coinciding with the direction of the passive objective rotation. Two ways to control the ion flux at the second stage of stabilization are considered and compared with each other: by changing the thrust of the ion engine and by turning the ion flow direction. For the first way it is supposed that the orientation system of the active spacecraft holds a constant deviation angle of the ion flux axis from the line connecting the centers of mass of the active spacecraft and the passive object. For the study, a mathematical model is developed that describes the motion of the system in the orbit plane and takes into account both the relative position of the passive object and the active spacecraft and the orientation of the object relative to the ion flux. Lyapunov's theorems on stability and asymptotic stability in the first approximation and Hamilton–Jacobi–Bellman equation [21] are used to build the control laws.

The self-similar model of ion engine plume expansion and fully diffused reflection model of ions interaction with the object's surface are used to calculate the effect of ion flow on the object [22,23]. It is assumed that the ion flow does not interact with the atmosphere and ionosphere plasma of the Earth. In addition, the influence of the atmosphere on the attitude motion of the passive object is neglected.

An ideal case of planar motion, which is a particular case of spatial motion, is considered in this paper. There are currently no studies on ion beam control aimed at detumbling and attitude stabilization of space debris. Spatial three-dimensional motion is described by complex mathematical models, the use of which is very difficult to identify the fundamental features of the considered mechanical system behavior. Consideration of the plane case allows one to grope the approaches to motion control, which can then be attempted to be transferred to a more complex three-dimensional case. Because plane motion is a special case of the three-dimensional, its analysis allows us to discard nonworking ideas without resorting to cumbersome calculations. Investigation of in-plane motion as the first step in studying the dynamics of a mechanical system has proven itself, for example, in the analysis of uncontrolled descent of reentry vehicles in the atmosphere [24].

Because the problem is considered in plane statement, restrictions on the shape of a passive object are imposed. It should have a plane of symmetry, which should lie in the plane of the orbital flight, and the center of mass of the passive object should be in the plane of symmetry. In the opposite case, the ion beam will create a moment tending to deflect the object out of the orbital plane. As a passive object, a cylindrical spent rocket stage is considered here.

This paper consists of six sections. Section II is devoted to the development of a mathematical model. Section III proposes the control law of the engine thrust and proves its asymptotic stability. Section IV builds control using the changing ion flow direction. Results of numerical simulations and comparison of control laws are given in Sec. V. Conclusions are presented in Sec. VI.

II. Mathematical Model

A. General Equations of Motion of a Mechanical System

The motion of a mechanical system consisting of space debris and an active spacecraft—"shepherd," which is equipped with two ion thrusters—is considered. It is assumed that the motion occurs in the orbital plane under the action of gravitational forces and the thrust force of the ion thrusters, and the force resulting from the ion beam impinging on the debris. The space debris is considered as a rigid body with a center of mass at point B, and the spacecraft is the material point A (Fig. 1). The system position can be described using five generalized coordinates: the true anomaly angle υ, the distance between the center of the Earth and the spacecraft r, distance between the spacecraft and the space debris center of mass d, angle of deviation of the line connecting the spacecraft and the center of mass of the space debris from the local horizon of the spacecraft α, and the space debris deflection angle θ. The direction of the axis of the ion flow created by the engine of the spacecraft can be defined by the angle β.

Before proceeding to the construction of the equations of motion, several coordinate systems should be introduced (Fig. 1): the inertial coordinate system Ox_py_p, orbital coordinate system Axy, body frame Bx_by_b, and ion-beam-related coordinate system Ax_ay_a. Origin O is the center of the Earth. The axis Ox_p passes through the pericenter of initial space debris orbit. The origin of the orbital frame Axy is located at the center of mass of the spacecraft. The axis Ax lies along the radius vector of the spacecraft. The axis Ay is directed toward the orbital flight. The body frame Bx_by_b is fixed relative to the space debris. The active spacecraft is a material point A. The axis Ax_a is directed along the ion beam axis to the flight direction, and the axis Ay_a completes the right-handed set.

To obtain the equations of the considered mechanical system motion, the second-kind Lagrange equations can be used:

$$\frac{d}{dt}\frac{\partial L}{\partial \dot{q}_j} - \frac{\partial L}{\partial q_j} = Q_j \tag{1}$$

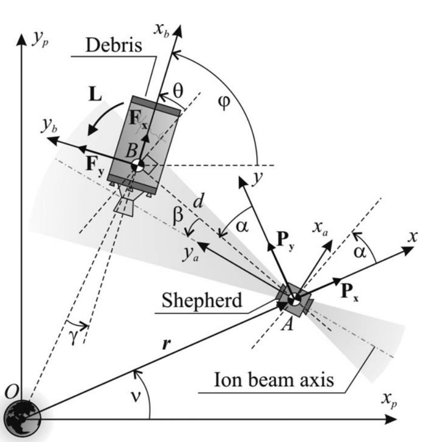

Fig. 1 Mechanical system.

where $L = T - U$ is the Lagrangian, T is the kinetic energy, U is the potential energy, Q_j is the nonpotential generalized forces, and q_j is a component of the generalized coordinates vector $\boldsymbol{q} = [r, v, d, \alpha, \theta]$. The kinetic energy of the system is the sum of the kinetic energy of the space debris and energy of the spacecraft:

$$T = \frac{m_A V_A^2}{2} + \frac{m_B V_B^2}{2} + \frac{I_z \dot{\varphi}^2}{2} \tag{2}$$

where m_A is the mass of the spacecraft; m_B is the mass of the space debris; $V_A = \dot{r}^2 + r^2\dot{v}^2$ is the velocity of the spacecraft; V_B is the velocity of the space debris, which will be written below; I_z is the transversal moment of inertia of the space debris; and $\varphi = v + \alpha + \theta$ is the angle of deviation of the longitudinal axis of space debris Bx_b from the axis Ox_p of the inertial coordinate system (Fig. 1). The potential energy of the system is the sum of the potential energy of the material point A and a rigid body with a center of mass at the point B in the central gravitational field of the Earth.

$$U = -\frac{\mu m_A}{r} - \frac{\mu m_B}{r_B} - \frac{\mu(I_x + I_y + I_z)}{2r_B^3} + \frac{3\mu(I_x \cos^2\gamma + I_y \sin^2\gamma + I_z)}{2r_B^3} \tag{3}$$

where μ is the gravitational constant of the Earth, $r_B = OB$ is the distance from the center of the Earth to the center of mass of the space debris, I_x is the longitudinal moment of inertia of the space debris, I_y is the transversal moments of inertia of the space debris, $\gamma = \theta + \alpha - \eta$ is the deflection angle of the longitudinal axis of space debris Bx_b from its local vertical OB (Fig. 2), and $\eta = \arctan(BE/OE) = \arctan(d\cos\alpha/r - d\sin\alpha)$. Since $d \ll r$, angle η can be expanded into series $\eta \approx (d/r)\cos\alpha + O((d/r))^2$, and it can be roughly assumed that $\gamma \approx \theta + \alpha$.

To determine the distance r_B and velocity V_B, the coordinates of point B in the inertial coordinate system should be written

$$x_B = r\cos v - d\sin(\alpha + v), \quad y_B = r\sin v + d\cos(\alpha + v) \tag{4}$$

The distance r_B can be written in the form

$$r_B = \sqrt{x_B^2 + y_B^2} = \sqrt{r^2 - 2dr\sin\alpha + d^2} \tag{5}$$

After calculating the derivative of the coordinates (4) the square of the velocity V_B can be found as

$$V_B^2 = \dot{x}_B^2 + \dot{y}_B^2 = \dot{r}^2 + \dot{d}^2 + d\dot{\alpha}^2 + 2d^2\dot{\alpha}\dot{v} + \dot{v}^2(r^2 + d^2) + 2\cos\alpha(\dot{d}r\dot{v} - d\dot{r}\dot{v} - d\dot{\alpha}\dot{r}) - 2\sin\alpha(dr\dot{\alpha}\dot{v} + dr\dot{v}^2 + \dot{d}\dot{r}). \tag{6}$$

During the motion, nonpotential forces act on the mechanical system: spacecraft control engine's thrust force projections P_x and P_y; the ion beam force arising from the ion flow blowing the space debris, and presented in the form of two projections on the axes of the body coordinate system F_x and F_y; and the torque L_z from the ion beam. Taking into account these forces and torque, the generalized nonpotential forces can be written as

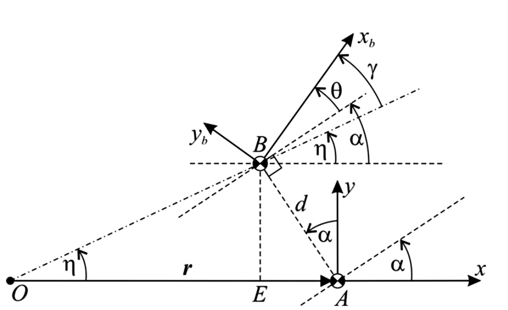

Fig. 2 Determination of angles.

$$Q_r = P_x + F_x\cos(\alpha + \theta) - F_y\sin(\alpha + \theta) \tag{7}$$

$$Q_v = P_y + F_x(r\sin(\alpha + \theta) - d\cos\theta) + F_y(r\cos(\alpha + \theta) + d\sin\theta) + L_z \tag{8}$$

$$Q_d = F_x\sin\theta + F_y\cos\theta \tag{9}$$

$$Q_\alpha = d(F_y\sin\theta - F_x\cos\theta) + L_z \tag{10}$$

$$Q_\theta = L_z \tag{11}$$

Substitution of Eqs. (2) and (3) into Eq. (1) taking into account Eqs. (4–11) and some simplifications gives

$$\ddot{r} = -\frac{\mu}{r^2} + r\dot{v}^2 + \frac{P_x}{m_A} \tag{12}$$

$$\ddot{v} = -\frac{2\dot{r}\dot{v}}{r} + \frac{P_y}{rm_A} - \frac{3\mu(I_x - I_y)\sin(2(\alpha + \theta))}{2r^2 m_A r_B^3} \tag{13}$$

$$I_z(\ddot{v} + \ddot{\alpha} + \ddot{\theta}) + \frac{3\mu(I_y - I_x)\sin(2(\alpha + \theta))}{2r_B^3} = L_z \tag{14}$$

$$\begin{aligned}\ddot{d} = &-\frac{\mu\sin\alpha}{r^2} + \frac{P_x\sin\alpha - P_y\cos\alpha}{m_A} + d\dot{\alpha}^2 + 2d\dot{\alpha}\dot{v} + d\dot{v}^2 \\ &+ \frac{F_x\sin\theta + F_y\cos\theta}{m_B} + \frac{\mu(r\sin\alpha - d)}{r_B^3} \\ &- \frac{3\mu(I_x - I_y)(\sin(3\alpha + 2\theta) + \sin(\alpha + 2\theta))}{4r_B^3 m_A r} \\ &- \frac{3\,\mu r}{8m_B r_B^5}(3(I_x - I_y)(\sin(3\alpha + 2\theta) \\ &- \sin(\alpha + 2\theta)) + 2(I_x + I_y + 4I_z)\sin\alpha) \\ &+ \frac{3\mu(3d(I_x - I_y)\cos(2\alpha + 2\theta) + d(I_x + I_y + 4I_z))}{4m_B r_B^5}\end{aligned} \tag{15}$$

$$\begin{aligned}\ddot{\alpha} = &-\frac{\mu\sin\alpha}{r^2} + \frac{2\dot{r}\dot{v}}{r} - \frac{2\dot{d}(\dot{\alpha} + \dot{v})}{d} + \frac{F_y\sin\theta - F_x\cos\theta}{dm_B} \\ &+ \frac{P_x\cos\alpha + P_y\sin\alpha}{dm_A} - \frac{P_y}{rm_A} + \frac{3\mu(I_x - I_y)\sin(2\alpha + 2\theta)}{2r_B^3 rm_A} \\ &+ \frac{\mu r\cos\alpha}{r_B^3 d} - \frac{3\mu(I_x - I_y)(\cos(\alpha + 2\theta) - \cos(3\alpha + 2\theta))}{4r_B^3 rdm_A} \\ &- \frac{3\,\mu r((I_x - I_y)(\cos(\alpha + 2\theta) + \cos(3\alpha + 2\theta)) + 2(I_x + I_y + I_z)\cos\alpha)}{8r_B^5 dm_B}\end{aligned} \tag{16}$$

Equations (12) and (13) describe the motion of a spacecraft. Equation (14) describes the motion of space debris relative to its center of mass. Equations (15) and (16) describe the motion of the center of mass of the space debris.

B. Calculation of the Ion Beam Forces and Torque

For calculation ion beam forces F_x and F_y and torque L_z the self-similar model of ion engine plume expansion and fully diffused reflection model of ions interaction with the surface can be used. The self-similar model assumes that all streamlines expand similarly and the ion flow expansion can be described through a dimensionless self-similarity function, which determines the concentration of ions in the ion beam. A detailed description of this model can be found in [22,23]. The surface of the space debris can be divided into triangles, and the force acting on each jth triangle can be calculated. The self-similar model allows calculating the density of ions near the surface of each triangle.

$$\boldsymbol{F}_j = -\frac{m_0 n_0 R_0^2 S_j V_0^2}{x_{aj}^2 \tan^2\alpha_0} \exp\left(-\frac{3(y_{aj}^2 + z_{aj}^2)}{x_{aj}^2 \tan^2\alpha_0}\right)(\boldsymbol{e}_{Vj} \cdot \boldsymbol{N}_j)\boldsymbol{e}_{Vj} = V_0^2 \bar{\boldsymbol{F}}_j \tag{17}$$

where m_0 is the ion mass; n_0 is the plasma density at the beginning of the far region; R_0 is the radius of the beam at the beginning of the far region; α_0 is the divergence angle of the ion beam; $\boldsymbol{e}_{Vj} = [-1, -y_{aj}x_{aj}^{-1}, -z_{aj}x_{aj}^{-1}]^T$ is the vector directed along the velocity of the ion flux at the barycenter P_j of jth triangle, given by its coordinates in the $Ax_a y_a z_a$ frame (Fig. 1); V_0 is the axial component of the ion flux velocity; the radius vector of the barycenter point P_j in the $Ax_a y_a z_a$ frame has coordinates $\boldsymbol{\rho}_j = [-x_{aj}, y_{aj}, z_{aj}]^T$; S_j is the area of jth triangle; and $\bar{\boldsymbol{F}}_j$ is the ion beam force divided by square axial component of the ion flux velocity. Then the summation is performed, and the resultant force and moment acting on the whole body are calculated.

$$\boldsymbol{F} = \sum_{j\in J}\boldsymbol{F}_j = V_0^2\sum_{j\in J}\bar{\boldsymbol{F}}_j, \quad \boldsymbol{L} = \sum_{j\in J}\boldsymbol{\rho}_j \times \boldsymbol{F}_j = V_0^2\sum_{j\in J}\boldsymbol{\rho}_j \times \bar{\boldsymbol{F}}_j \tag{18}$$

where J is an index set including the subset of triangles inside the ion beam. The ion force and moment depend on many parameters, in particular, on the distance d, angles θ and β, and the location of the center of mass inside the body. The force transmitted by the ion beam is proportional to the square of the ion flux velocity V_0, which can be controlled over a wide range by the voltage inside the ion engine. Denote by $V_0^{\max}$ is the maximum axial component of the ion flux that the ion engine can provide. If the engine does not operate at full capacity, then it creates a flow of ions at a speed of $V_0 = \sqrt{u}V_0^{\max}$, where u is a weighting factor, which characterizes the power of the engine, and can vary in the range from 0 to 1. Then ion beam torque of the engine that is not operating at full power can be represented as

$$\boldsymbol{L} = u\boldsymbol{L}^{\max} \tag{19}$$

where $\boldsymbol{L}^{\max} = (V_0^{\max})^2 \sum_{j\in J}\boldsymbol{\rho}_j \times \bar{\boldsymbol{F}}_j$.

If the ion beam force $\boldsymbol{F}$ is calculated, then the ion beam torque relative to the space debris center of mass $\boldsymbol{L}$ can be written as

$$\boldsymbol{L} = \boldsymbol{r}_p \times \boldsymbol{F} \tag{20}$$

where $\boldsymbol{r}_p$ is the vector connecting the center of mass with the point of the ion beam resulting force application. Vector $\boldsymbol{r}_p$ is not constant. It depends on the ion flow parameters and the orientation of the space debris. An analogy with aerodynamic moments can be made here, because the aerodynamic force is applied not in the center of mass of a body, but in the center of pressure.

C. Case of the System Motion in a Circular Orbit

Two types of control will be discussed below: changing the speed of the ion flux and changing the angle of deflection of the axis of the ion flow. A particular case when motion occurs in a circular orbit is considered.

$$r = \text{const}, \qquad \dot{\upsilon} = \omega = \sqrt{\mu r^{-3}} \tag{21}$$

The relative position of space debris is held constant by the control system of the spacecraft. In this case

$$\alpha = 0, \qquad \dot{\alpha} = 0, \qquad d = \text{const} \tag{22}$$

After the transition to a new independent variable, $\tau = \sqrt{2}\Omega t$, and taking into account Eq. (19), the equation of the space debris attitude motion (14) can be written in the form

$$\theta'' + \frac{1}{2}\sin 2\theta = \frac{u(\theta, \theta')L_z^{\max}}{2\Omega^2 I_z} \tag{23}$$

where $\Omega^2 = [3\mu(I_y - I_x)/2r^3 I_z] > 0$, $u(\theta, \theta') = [0, 1]$ is the dimensionless control parameter, $L_z^{\max}$ is the ion beam torque created by the included at full power ion engine, and the prime means the derivative with respect to the variable τ. From a physical point of view, the control parameter $u(\theta, \theta')$ is proportional to the square rate of discharge of ions and is determined by the voltage in the ion engine $u = (V_0/V_0^{\max})^2$. Because the ion engine cannot inhale the ions inward, this control parameter is positive. After expansion of the ion beam torque into the Fourier series

$$L_z^{\max}(\theta) = a_0 + \sum_{j=1}^{\infty}(a_j \cos j\theta + b_j \sin j\theta) \tag{24}$$

the equation describing the motion of space debris relative to its center of mass can be obtained in the form

$$\theta'' + \frac{1}{2}\sin 2\theta = \frac{u(\theta, \theta')}{2\Omega^2 I_z}\left(a_0 + \sum_{j=1}^{\infty}(a_j \cos j\theta + b_j \sin j\theta)\right) \tag{25}$$

where a_i and b_i are the Fourier coefficients. This equation will be used in the following section to find control laws that stabilize the space debris attitude motion in the position $\theta = 0$.

III. Space Debris Attitude Control by Changing the Thrust of the Ion Engine

A. Thrust Control on a Circular Orbit

The case when the orientation system of the active spacecraft holds a constant deviation angle of the ion beam axis from the line connecting the centers of mass of the active spacecraft and the space debris β = const all the time is considered. Function $L_z^{\max}(\theta)$ view is greatly influenced by the space debris center of mass position and the deviation angle β.

Consider a situation of uncontrolled motion, when the engine is turned on at full power ($u = 1$). In the particular case when the space debris center of mass lies in the plane of symmetry (Fig. 3 dash dotted line), its torque $L_z^{\max}$ is an odd function of the angle θ for $\beta = 0$. Figures in this subsection is plotted for cylindrical space debris, whose length is $l = 6.5$ m, radius is 1.2 m, and the center of mass is shifted 0.2 m to the bottom. Equation (23) has an equilibrium position $\theta = 0$, $\theta' = 0$, since $L_z^{\max}(0) = 0$. For this case, the following expressions for the Fourier series coefficients (24) can be written: $a_j = 0$. In the general case, when the center of mass does not lie in the symmetry plane, the value $\theta = 0$ is not the root of the function $L_z^{\max}(\theta)$ for $\beta = 0$ (Fig. 3 dotted line), and $\theta = 0$, $\theta' = 0$ is not the equilibrium position of Eq. (23). Changing the angle β leads to a change in the graph of the function $L_z^{\max}(\theta)$. A series of calculations showed that, for a cylindrical body, the value $\beta = \beta^*$ can be found such that $L_z(0) = 0$ (Fig. 3 solid line). In this case $\theta = 0$ is equilibrium position of Eq. (23), and the following relation can be written for the coefficients of the Fourier series (24): $\sum_{j=0}^{\infty} a_j = 0$. The next subsection (Sec. B) is devoted to the construction of control law for stabilizing oscillations in the position $\theta = 0$ for this general case when $\beta = \beta^*$.

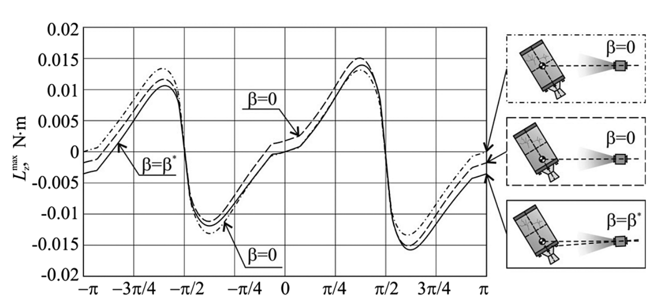

Fig. 3 Dependence of the ion beam torque on the angle of the space debris deflection θ for various positions of the center of mass and the angles of the ion beam axis deviation β.

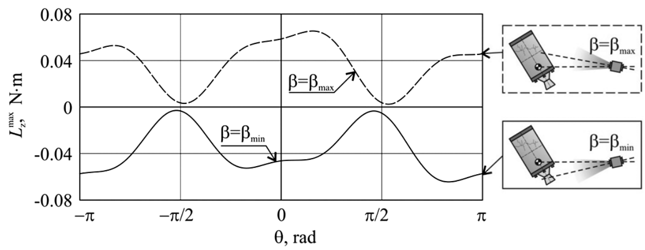

Fig. 4 Dependence of the ion beam torque on the angle of the space debris deflection θ for various angles of the ion beam axis deviation β.

Cases when the ion beam axis is deflected by an angle $\beta_{\max}$ or $\beta_{\min}$, providing a maximum or minimum of ion beam torque at the point $\theta = 0$, should be also considered (Fig. 4), because a larger modulus of torque allows to expect faster stabilization, wherein the control law $u(\theta, \theta')$ should be selected so that $\theta = 0$, $\theta' = 0$ is the equilibrium position of Eq. (23). This case is considered in Sec. C.

Ion engine thrust control for two cases will be considered below. In the first case ($\beta = \beta^*$), the function $L_z^{\max}(\theta)$ becomes zero at the point $\theta = 0$, and the function changes sign when passing through this point. In the second case ($\beta = \beta_{\min}$ or $\beta = \beta_{\max}$), function $L_z^{\max}(\theta)$ does not equal to zero at the point $\theta = 0$ and its neighborhood. The laws of the ion engine thrust control that are being developed are based on the idea that the torque created by the engine should be directed against the angular velocity of rotation of the space debris.

B. Thrust Control for the Case when $L_z^{\max}(0) = 0$ ($\beta = \beta^*$)

It is proposed to use the control in the form

$$u = \begin{cases} -2k\Omega^2 I_z \theta\theta', & \text{when } \theta\theta' < 0, \\ 0, & \text{when } \theta\theta' \geq 0 \end{cases} \tag{26}$$

where k is the constant control parameter, which is chosen from the condition $u < 1$. To maximize control impact, the control parameter should be chosen as

$$k = \frac{1}{2\Omega^2 I_z \max(|\theta\theta'|)} \tag{27}$$

Because the amplitude of the angle oscillations and its angular velocity decrease as the equilibrium position is approached, it is advisable to periodically recalculate this coefficient. For example, at the moment when $\theta = 0$ and $\theta' > 0$ the coefficient k could be recalculated on the basis of data for the previous period of the angle θ oscillation.

Consider the mechanism of operation of the control law $u = -2k\Omega^2 I_z \theta\theta'$ in the absence of the constraint $u > 0$. Consider the ion beam torque $L_z^{\max}$ of a full-powered engine acting on the space debris. The period of its oscillations can be divided into four zones (Fig. 5). The dashed line shows oscillations without control, when $u = 1$ and $L_z = L_z^{\max}$. The solid line demonstrates controlled motion. At zones I and III, the direction of the torque $L_z^{\max}$ coincides with the direction of the space debris rotation (Fig. 6). This torque tends to increase the angular velocity of rotation. To slow down the rotation of the space debris, the direction of the torque must be changed to the opposite. Therefore, the control parameter u must be negative. In this case $\mathrm{sign}(L_z) = -\mathrm{sign}(L_z^{\max})$. At zones II and IV, the direction of the space debris rotation and the ion beam torque $L_z^{\max}$ do not coincide. In this case, the torque slows down the rotation, and the control coefficient u should be positive. In this case $\mathrm{sign}(L_z) = \mathrm{sign}(L_z^{\max})$. Thus, the idea is that the control parameter u is chosen so that the product $u(\theta, \theta')L_z^{\max}$ has a sign opposite to the angular velocity θ'. Figure 7 demonstrates schematically the position and direction of the space debris rotation. In a real situation, when control $u < 0$ is not physically feasible, the ion engine is turned off (in zones I and III), in order to not accelerate the rotation of the space debris.

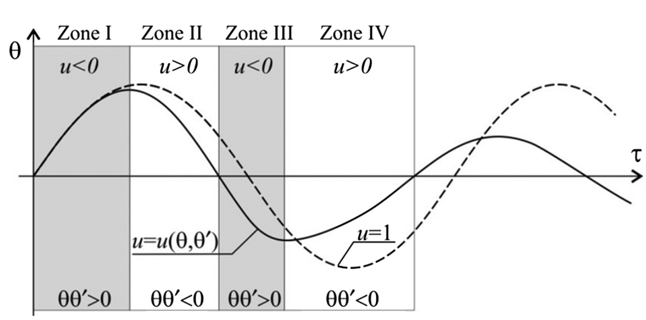

Fig. 5 Space debris oscillation.

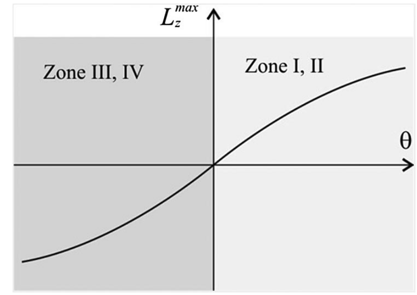

Fig. 6 Ion beam torque.

Two cases will be considered separately, when control $u = -2k\Omega^2 I_z \theta\theta'$ is implemented and when $u = 0$. We first reject the constraint $u > 0$ and show that the control $u = -2k\Omega^2 I_z \theta\theta'$ can provide the asymptotic stability of the equilibrium position $\theta = 0$, $\theta' = 0$. To study the stability, we use the first approximation approach [25]. It is assumed that θ and θ' are small values of the ε order. The expansion in Eq. (19) of trigonometric functions in series gives

$$\theta'' + \theta - \frac{2}{3}\theta^3 + \frac{2}{15}\theta^5 + \cdots = -k\theta\theta'(c_0 + c_1\theta + c_2\theta^2 + c_3\theta^3 + c_4\theta^4 + c_5\theta^5 + \cdots)$$

Transferring the nonlinear terms in the right side of the equation gives

$$\begin{aligned} \theta'' + \theta &= -k\theta\theta'(c_0 + c_1\theta + c_2\theta^2 + c_3\theta^3) \\ &\quad + \frac{2}{3}\theta^3 - \frac{2}{15}\theta^5 + O(\varepsilon^6) \end{aligned} \tag{28}$$

where $c_0 = \sum_{j=0}^{n} a_j = 0$, $c_1 = \sum_{j=1}^{n} j b_j$, $c_2 = -(1/2)\sum_{j=1}^{n} (j)^2 a_j$, and $c_3 = -(4/3)\sum_{j=1}^{n} (j/2)^3 b_j$ are the coefficients of the ion beam torque decomposition. In the case $L_z(0) = 0$, the coefficient $c_0 = 0$. Equation (28) can be written in the matrix form

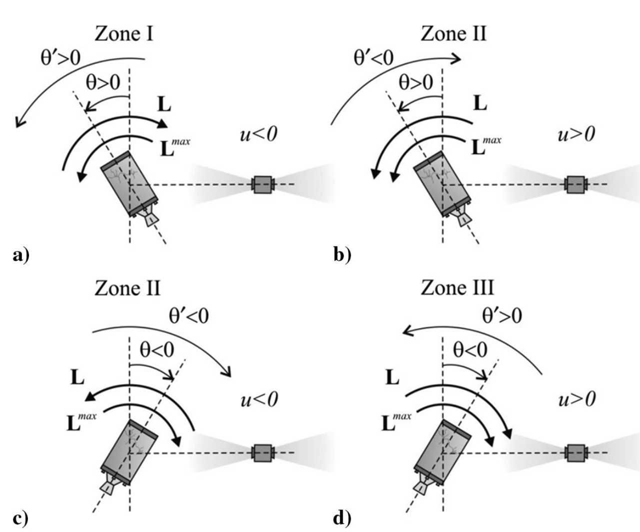

Fig. 7 Ion beam torque L in different phases of the oscillation period.

$$x' = Ax + g(x) \tag{29}$$

where $\boldsymbol{x} = [x_1, x_2]^T$ is the vector, $x_1 = \theta'$, $x_2 = \theta$, $\boldsymbol{A} = \begin{bmatrix} 0 & -1 \\ 1 & 0 \end{bmatrix}$, $\boldsymbol{g} = [g_1, g_2]^T$ is the nonlinear terms vector, $g_j = \sum_{k=1}^{n} g_j^{(k)}$, $g_i^{(j)}$ is the function that contains the variables of kth order, $g_1^{(2)} = g_2^{(2)} = g_2^{(3)} = 0$, and $g_1^{(3)} = -kc_1x_1x_2^2 - (2/3)x_2^3$. The matrix $\boldsymbol{A}$ has two purely imaginary eigenvalues $\pm i$. This is the simplest critical case described in section 29.b of the book [25]. The conclusion about the stability of the equilibrium position cannot be made on the basis of the analysis of the linear system $\boldsymbol{x}' = \boldsymbol{A}\boldsymbol{x}$. For stability analysis, it is necessary to take into account the contribution of nonlinear expansion terms. Following the methodology given in [25], the Lyapunov function for the equation containing terms of order ε^3 will be searched in the form

$$V = x_1^2 + x_2^2 + \frac{1}{3}x_1^4 + \frac{2}{3}x_1^2x_2^2 + x_1x_2(x_1^2 - x_2^2)\gamma_4 \tag{30}$$

where $\gamma_4 = -(kc_1/4)$. The total derivative $\dot{V}$ for Eq. (29) is

$$\dot{V} = \gamma_4(x_1^2 + x_2^2)^2 + O(\varepsilon^7) \tag{31}$$

Taking into account the smallness of the values of x_j, it can be concluded that the Lyapunov function V given by Eq. (30) is positive definite (Fig. 8) at small values x_1 and x_2, and its derivative $\dot{V}$ given by Eq. (31) is positive definite when $\gamma_4 > 0$, and negative definite when $\gamma_4 < 0$ (Fig. 9). In other words the equilibrium is asymptotically stable in the case where $\gamma_4 < 0$, and unstable in the case $\gamma_4 > 0$. Thus, the condition for the asymptotic stability of the equilibrium state can be written as

$$kc_1 > 0 \tag{32}$$

Consider now the case when $u = 0$. The Lyapunov function for Eq. (25) in this case can be written in the form

$$V = \theta'^2 + (2 - \cos^2\theta) \tag{33}$$

The derivative of function (33), taking into account Eq. (25) with $u = 0$, is identically zero.

$$\dot{V} = 0$$

According to the Lyapunov stability theorem, the equilibrium state $\theta = 0$, $\theta' = 0$ is stable.

The use of control (26) allows transferring the phase trajectory to a neighborhood of the equilibrium position $\theta = 0$, $\theta' = 0$. When $\theta\theta' < 0$, the trajectory approaches the equilibrium position due to its asymptotic stability, and when $\theta\theta' > 0$, the trajectory does not move away from the equilibrium position due to its stability. Thus, control (26) consistently approximates the phase trajectory to the equilibrium position.

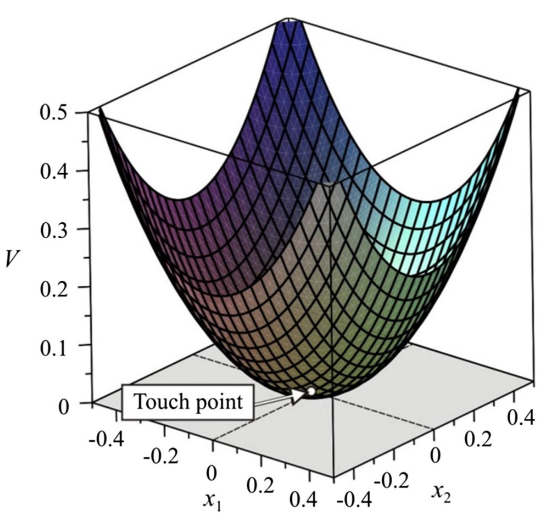

Fig. 8 Lyapunov function (30) for $\gamma_4 = -0.2$.

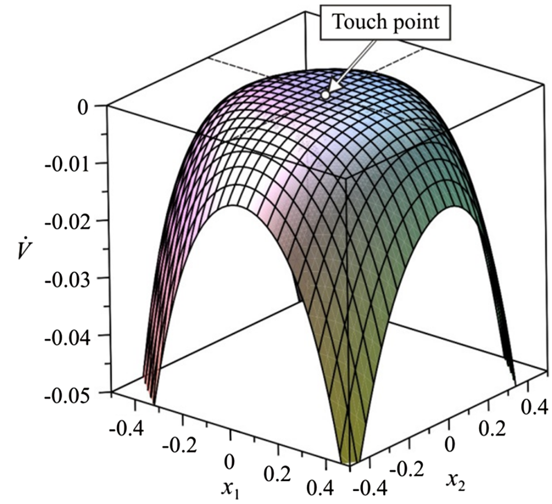

Fig. 9 Lyapunov function derivative (31) for $\gamma_4 = -0.2$.

C. Thrust Control for the Case when $L_z^{\max}(0) \neq 0$ ($\beta = \beta_{\min}$ or $\beta = \beta_{\max}$)

Consider the case when the ion flux torque does not become zero in the vicinity of the point $\theta = 0$. The following control law is proposed:

$$u(\theta') = -2k\Omega^2 I_z \theta' \tag{34}$$

where $\mathrm{sign}(k) = \mathrm{sign}(L_z^{\max}(0))$. Because in the considered case the function $L_z^{\max}$ does not change its sign, the torque when using the control (34) is always directed opposite to the direction of rotation and slows it down. In this case, the equation of motion takes the form

$$\theta'' + \frac{1}{2}\sin 2\theta = -k\theta'\left(a_0 + \sum_{j=1}^{n}(a_j\cos j\theta + b_j \sin j\theta)\right) \tag{35}$$

To prove that the equilibrium position $\theta = 0$, $\theta' = 0$ is asymptotically stable, we use the first approximation approach. After expanding Eq. (35) in a series in the point $\theta = 0$, the result can be written in matrix form (29), where $\boldsymbol{A} = \begin{bmatrix} -kc_0 & -1 \\ 1 & 0 \end{bmatrix}$, $\boldsymbol{g} = \begin{bmatrix} -k\theta'(c_1\theta + c_2\theta^2 + c_3\theta^3 + \cdots) + \frac{2}{3}\theta^3 - \frac{2}{15}\theta^5 \\ 0 \end{bmatrix}$, $c_0 = \sum_{j=0}^{n} a_j$. The eigenvalues of matrix A have the form

$$\lambda_{1,2} = -\frac{kc_0}{2} \pm \sqrt{\left(\frac{kc_0}{2}\right)^2 - 1} \tag{36}$$

The equilibrium position $\theta = 0$, $\theta' = 0$ is asymptotically stable regardless of nonlinear terms $\boldsymbol{g}(\boldsymbol{x})$ if the real parts of all eigenvalues (36) are less than zero. This condition is satisfied if

$$kc_0 > 0 \tag{37}$$

Condition (37) is satisfied when the above ratio $\mathrm{sign}(k) = \mathrm{sign}(L_z^{\max}(0)) = \mathrm{sign}(c_0)$ is true.

IV. Space Debris Attitude Control by Changing the Direction of the Ion Flow

As mentioned above, the ion beam torque L_{iz} depends on the angle of deflection of the axis of ion beam (angle β in Fig. 1). In this section, the task of stabilizing space debris attitude motion in a circular orbit by changing β is considered. The task of finding the time-optimal control that transfers the system to the equilibrium position is posed to determine control structure. The controlled motion equation can be written as

$$\theta'' + \frac{1}{2}\sin 2\theta = w(\theta, \beta) \tag{38}$$

where $w(\theta, \beta) = [L_z(\theta, \beta)/2\Omega^2 I_z]$ is the control function. The cost function is

$$J = \int_0^{t_k} \mathrm{d}t \tag{39}$$

For Eq. (38) and cost function (39), the Hamilton–Jacobi–Bellman equation can be written in the form [26]

$$\min_{w\in[w_{\min};w_{\max}]}\left[\frac{\partial\varphi^B(\tau,\theta,\theta')}{\partial\tau} + \frac{\partial\varphi^B(\tau,\theta,\theta')}{\partial\theta}\theta' + \frac{\partial\varphi^B(\tau,\theta,\theta')}{\partial\theta'}\left(-\frac{1}{2}\sin 2\theta + w\right) + 1\right] = 0 \tag{40}$$

where $\varphi^B(\tau, \theta, \theta')$ is unknown value function.

Because all the trajectories must reach the point $\theta = 0$, $\theta' = 0$ at the moment $\tau = t_k$, the boundary condition is defined only at this point $\varphi^B(T, \theta, \theta') = 0$. In accordance with the Bellman method, the structure of the optimal control can be found from the condition of the minimum of the expression in brackets in Eq. (40):

$$w = \begin{cases} w_{\max}, & \text{when } \frac{\partial\varphi^B(\tau,\theta,\theta')}{\partial\theta'} \le 0; \\ w_{\min}, & \text{when } \frac{\partial\varphi^B(\tau,\theta,\theta')}{\partial\theta'} > 0 \end{cases} \tag{41}$$

Equation (41) shows that optimal control is relay. An attempt to solve Eq. (30) makes it necessary to calculate the integral

$$\varphi^B(\tau,\theta,\theta') = -\int_{\theta_0}^{\theta}\frac{dx}{\sqrt{2w(x-\theta) + 4(\cos(x/2) - \cos(\theta/2)}} + F(-2w\theta + \theta'^2 - 4\cos(\theta/2))$$

which is impossible to do analytically. Therefore, we focus on building simplified control.

Consider a relay control when the angle β changes instantly. This assumption is fully justified, because the period of oscillations of space debris without a control is about an hour and the engine axis can be rotated in seconds. If the space debris is in fast rotation mode and this assumption is not fulfilled, then it should be first transferred into oscillation mode. To slow down the rotation angular velocity, it is necessary to turn the axis of the ion beam to obtain the maximum torque that will slow down the rotation [11]. After the angular velocity decreases and the space debris goes into oscillation mode, relay control (41) can be used to stabilize it. Figure 4 demonstrates the dependence of the L_z on the angle of deviation of space debris θ for various values of β. The mass-geometric parameters of space debris are given in Sec. III.A. An analysis of Fig. 10 shows that the maximum values of the moment L_z correspond to an angle $\beta_{\max} = -10°$, and the minimum values correspond to an angle $\beta_{\min} = 9°$. With a further increase in the angle modulus, the moments decrease as part of the passive object goes beyond the flow.

Using the dependences of the moment L_z on the angle θ shown in Fig. 4, the phase portrait of Eq. (23) for $\beta = \beta_{\min}$, $\beta = \beta_{\max}$ was constructed (Fig. 11). Solid lines show phase trajectories corresponding to $\beta = \beta_{\min}$, and dashed lines demonstrate phase trajectories for the case $\beta = \beta_{\max}$. Analysis of phase portrait shows that the transition to the equilibrium position $\theta = 0$, $\theta' = 0$ is possible either by phase trajectory I or by trajectory II (Fig. 11). Thus,

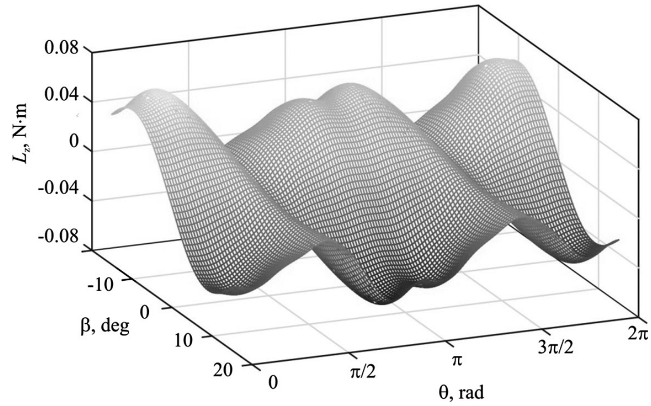

Fig. 10 Dependence of torque L_z on angle θ for various β.

the transition to the equilibrium position can be divided into two stages. First, it is required to transfer the phase point to the trajectory I or II, and then the point moves along this trajectory to the equilibrium position. Phase trajectories I and II divide the phase space into two areas. In the white zone to go to trajectory II we need to use control $\beta = \beta_{\max}$, and in the gray area we need to use control $\beta = \beta_{\min}$ to go to trajectory I. For example, if we are at point A in Fig. 11, then we need to rotate the ion beam axis by an angle $\beta = \beta_{\min}$; when we are in point B, we need to rotate the axis by angle $\beta = \beta_{\max}$. This will allow us to get to the point $\theta = 0$, $\theta' = 0$ along trajectory I. It should be noted that if at the initial moment of time the body oscillates at a relatively small amplitude around the equilibrium position $\pm\pi/2$, then it is required to turn off the engine and wait until the imaging point leaves the vicinity of this equilibrium position.

The described control requires obtaining an analytical equation for the phase trajectories I and II (Fig. 11). The solution of this problem causes difficulties in connection with complex nature of the moment L_z. The authors propose to use an approximate equation of the trajectory to determine the moment of control switching

$$\theta' = \pm\frac{1}{\Omega}\sqrt{\frac{L_0\theta}{I_z}} \tag{42}$$

where $L_0 = L_z(0)$ is the moment value corresponding to the equilibrium position $\theta = 0$. Taking into account Eq. (42), the following control can be offered:

$$\beta = \begin{cases} \beta_{\min}, & \text{when } \theta > -\frac{I_z\theta'^2\Omega^2}{L_0}\operatorname{sign}(\theta'), \\ \beta_{\max}, & \text{when } \theta < -\frac{I_z\theta'^2\Omega^2}{L_0}\operatorname{sign}(\theta') \end{cases} \tag{43}$$

When using control (43), the switching moment does not coincide with the optimal one; therefore, the transition to the equilibrium position is performed in more than one switching. Figure 12 shows schematically the phase trajectory and positions of space debris and active spacecraft at several points. At points D and H, control is switched. If we knew the analytical equation of the boundary, which

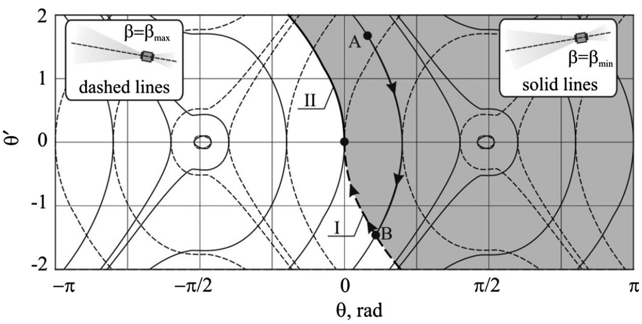

Fig. 11 Phase portrait.

Table 1 Fourier coefficients for various values of the ion flow axis deviation angle

	$\beta = \beta^* = 0.2036°$		$\beta = \beta_{\max} = -10°$		$\beta = \beta_{\min} = 9°$	
j	a_j, N · m	b_j, N · m	a_j, N · m	b_j, N · m	a_j, N · m	b_j, N · m
0	$-1.10158 \cdot 10^{-3}$	0	0.0368453	0	−0.0370000	0
1	$2.22337 \cdot 10^{-3}$	$-1.37822 \cdot 10^{-4}$	$6.24380 \cdot 10^{-3}$	$5.95066 \cdot 10^{-4}$	$6.01756 \cdot 10^{-3}$	$-1.11596 \cdot 10^{-3}$
2	$-8.89402 \cdot 10^{-4}$	$9.95015 \cdot 10^{-3}$	0.0242794	$7.52650 \cdot 10^{-3}$	−0.0237260	$7.71685 \cdot 10^{-3}$
3	$-7.20263 \cdot 10^{-4}$	$1.85450 \cdot 10^{-4}$	$1.54778 \cdot 10^{-4}$	$5.23968 \cdot 10^{-4}$	$-4.99732 \cdot 10^{-4}$	$-1.57499 \cdot 10^{-4}$
4	$2.83589 \cdot 10^{-4}$	$-5.53070 \cdot 10^{-3}$	$-8.98374 \cdot 10^{-3}$	$-1.07517 \cdot 10^{-3}$	$8.94706 \cdot 10^{-3}$	$-1.79172 \cdot 10^{-3}$
5	$4.03508 \cdot 10^{-4}$	$-1.52168 \cdot 10^{-4}$	$-3.60726 \cdot 10^{-4}$	$-5.47992 \cdot 10^{-4}$	$2.14785 \cdot 10^{-4}$	$5.89558 \cdot 10^{-4}$
6	$-8.73372 \cdot 10^{-5}$	$1.97856 \cdot 10^{-3}$	$2.95004 \cdot 10^{-4}$	$-1.71206 \cdot 10^{-3}$	$-8.13403 \cdot 10^{-4}$	$-1.32353 \cdot 10^{-3}$

is shown by a dashed line I, the transition from point A to the origin of coordinates could be done in one switch (near point D).

V. Results of Numerical Simulations

A. Parameters of the Mechanical System

As an example, an attitude motion of a Cosmos 3M [27] rocket stage in a circular orbit of 700 km altitude is considered. The stage has mass $m = 1400$ kg, its length is $l = 6.5$ m, and its radius is 1.2 m. The center of mass is shifted 0.2 m to the bottom of the rocket. The moments of inertia are $I_x = 1300\ \mathrm{kg \cdot m^2}$ and $I_y = I_z = 6800\ \mathrm{kg \cdot m^2}$. In this case $\Omega = 1.221 \cdot 10^{-3}$ rad/s The shepherd-spacecraft is held at a constant distance, $d = 15$ m, from the stage. It creates ion beam with the following parameters [28]: the mass of the particle (xenon) is $m_0 = 2.18 \cdot 10^{-25}$ kg, the plasma density is $n_0 = 2.6 \cdot 10^{16}\ \mathrm{m^{-3}}$, the radius of the beam at the beginning of the far region is 0.1 m, the axial component of the ion flux velocity $u_0 = 38000$ m/s, and the divergence angle of the beam is $\alpha_0 = 15°$. Figure 10 shows the dependence of the ion beam torque $L_z(\theta, \beta)$ that was obtained for the body and the flow with the above parameters using the calculation program developed by the authors [11]. Table 1 contains the values of the Fourier coefficients for various values of the deviation angle of the flow axis. Value $\beta^* = 0.2036°$ corresponds to the case $L_z^{\max}(0) = 0$, value $\beta = -10°$ corresponds to the maximum torque $L_z(\theta)$, and value $\beta = 9°$ corresponds to the minimum torque $L_z(\theta)$. Numerical simulation of attitude motion stabilization will be considered in the following section: when the space debris is in oscillation mode, and when the space debris is in rotation mode.

B. Atmospheric Impact Assessment

At low orbits magnitude of the aerodynamic forces and torques can be comparable with the values of the ion beam forces and torques. The study of the influence of the atmosphere on the motion of a Cosmos 3M rocket stage transported by an ion beam was carried out in [17]. For comparison of the aerodynamic and ion torques, the graphs of the maximum values of the torques on the altitude are shown in Fig. 13. The solid line shows the maximum aerodynamic torque L_{Az} acting on the rocket stage on a circular orbit. The dotted line corresponds to the moment of the ion beam $L_z = 0.0138$ N · m. The aerodynamic torque can be calculated as

$$L_{Az} = \frac{\rho(h) V_B^2}{2} S l \max(C_N) \tag{44}$$

where $\rho(h)$ is the atmospheric density at altitude h, $S = 4.524\ \mathrm{m^2}$ is the rocket's cross-sectional area, C_N is dimensionless aerodynamic coefficients of pitch moment, $\max(C_N) = 4.1$ [17], $V_B = \sqrt{\mu/(R_E + h)}$, and R_E is Earth radius. Calculations show that at an altitude of 500 km the maximum value of the aerodynamic torque is almost an order of magnitude smaller than the ion beam torque. At an altitude of about 651 km, the difference is two orders of magnitude. In this study, we will neglect the effect of the aerodynamic moment on the rocket, considering it to be small compared with the ion flux. In this study, the effect of the aerodynamic moment on the rocket is neglected as small compared with the ion beam torque. However, at low heights, the influence of the atmosphere must be taken into account, which may be the subject of future research.

C. Stabilization of the Space Debris Oscillations

The case when space debris is in oscillation mode is considered here. It is assumed that in the initial moment the following initial conditions are given: $\theta_0 = 0.5$ rad and $\theta_0' = 0$. The numerical integration of differential equation (25) was carried out using various ion engine's thrust control laws. In the first case (a thin solid line in Fig. 14), the ion beam axis was deflected by an angle $\beta = \beta^* = 0.2036°$, and control law (26) was used. After each half-cycle of oscillations, the control coefficient k was recalculated according to Eq. (27). The dependence of control $u(\theta, \theta')$ on an independent variable τ is shown in Fig. 15. The control does not reach the maximum value of 1, because it is proportional to the amplitude of angle θ oscillations, which decreases as a result of the control. In the second case (dashed line in Fig. 14), the beam axis is deflected by an angle $\beta_{\max} = -10°$, which provides the maximum modulus of ion beam torque $L_z^{\max}$ at $\theta = 0$, and the control law (26) was used. Figure 16 shows that the implementation of this law (dashed curve) requires significantly less engine thrust than that in the first case. In the third case (a thick solid line in Fig. 14), the axis is

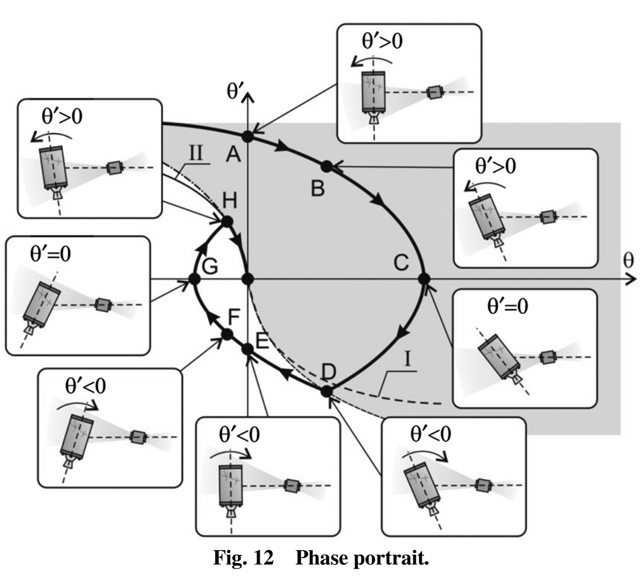

Fig. 12 Phase portrait.

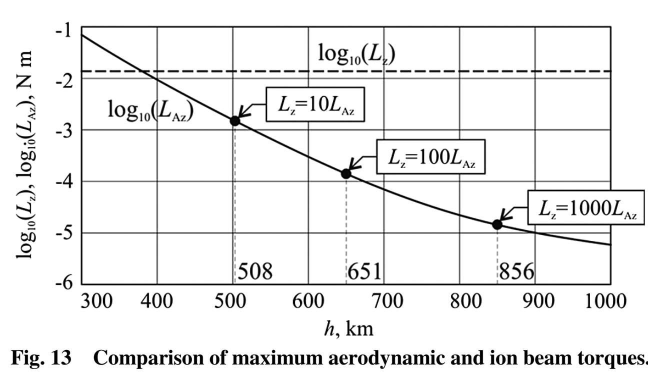

Fig. 13 Comparison of maximum aerodynamic and ion beam torques.

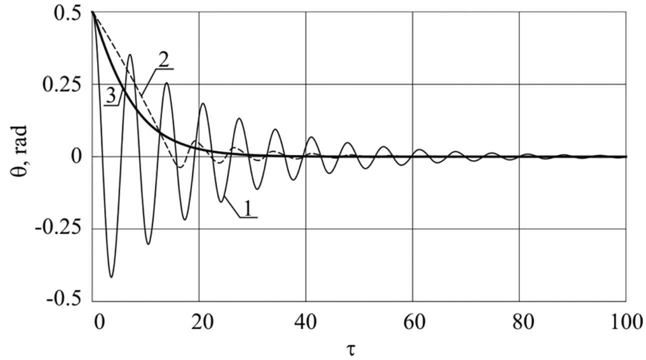

Fig. 14 Changing the space debris deflection angle θ using ion engine's thrust control.

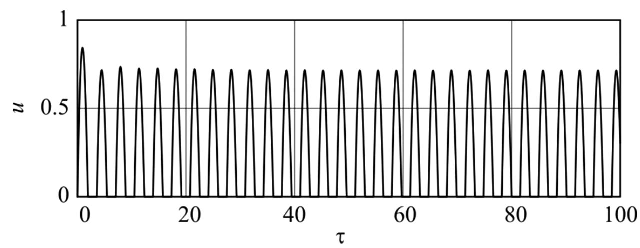

Fig. 15 Control law for the first case when $\beta = \beta^*$ and $u(\theta,\theta')$ is given by Eq. (26).

deflected by an angle $\beta_{\max} = -10°$ and the control law is given by Eq. (34). The control law is shown in Fig. 16 by a solid line (curve 3).

The results show that the third control law is most effective in terms of stabilization rates, whereas the first law is the least effective. In the first case, the angle passes into the ε-neighborhood of the equilibrium position $\theta = 0$ in 163,658 s (45 h, 27 minutes, and 38 s). In the second case, this process takes 101,572 s (28 h, 12 minutes, and 52 s). In the third it takes just 51,508 s (14 h, 18 minutes, and 28 s). In the calculations, it was chosen that $\varepsilon = 10^{-6}$.

Consider the stabilization of space debris by changing the angle of the ion beam axis deviation β. The result of integrating equation (38) with the control (43) is shown in Fig. 17. The law of the ion beam axis deviation angle is shown in Fig. 18. Calculations show that this law makes it possible to stabilize space debris by transferring it to the ε-neighborhood of the point $\theta = 0, \theta' = 0$ in 524 s, which is 8 minutes and 44 s.

Thus, controlling the orientation of the ion beam axis allows stabilization of the oscillations of space debris almost a hundred times faster than that in the case of ion engine thrust control.

D. Space Debris Detumbling

A situation where space debris rotates relative to its center of mass is considered in this subsection. It is assumed that at the initial time the following initial conditions are satisfied: $\theta_0 = 0$ and $\theta_0' = 105.5$ (this value corresponds to angular velocity $\dot{\theta}_0 = 10$ deg/s).

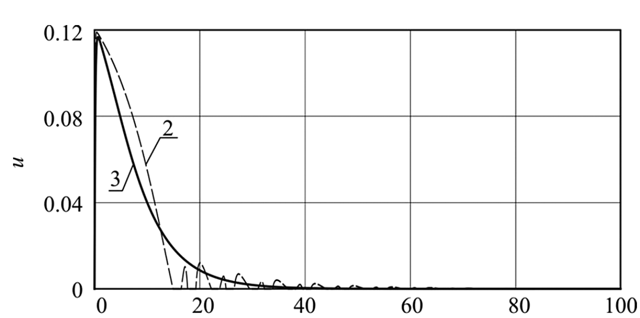

Fig. 16 Control law for the cases when $\beta = \beta_{\max}$ and $u(\theta,\theta')$ is given by Eq. (26) (curve 2) or by Eq. (34) (curve 3).

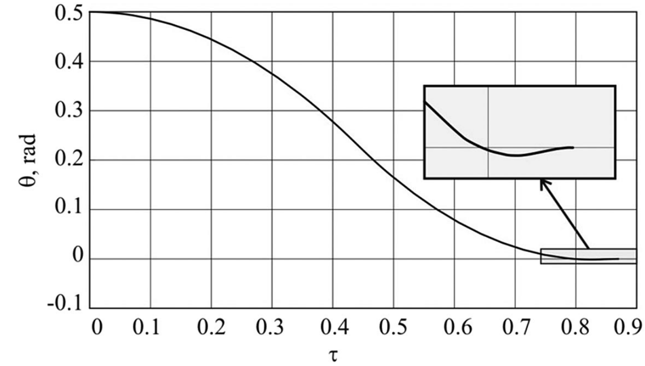

Fig. 17 Changing the space debris deflection angle θ using ion beam axis deflection control.

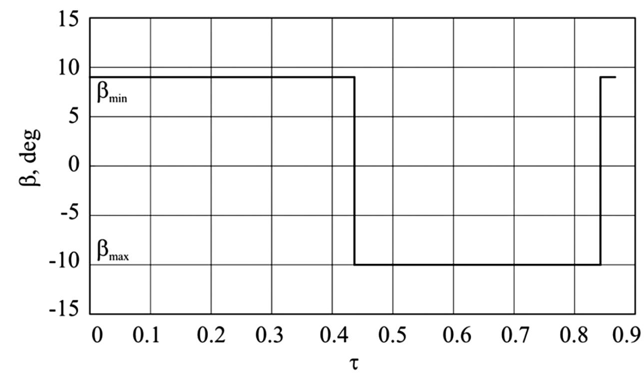

Fig. 18 Ion beam axis deflection angle control.

Researches [29,30] show that space debris can move at such angular velocities. As in the previous subsection, two methods of space debris attitude motion control are considered: by changing the ion engine thrust and by controlling the inclination of the ion beam axis.

Consider space debris detumbling by ion engine thrust control. The simulations show that the use of control law (26) does not allow stopping the rotation of space debris, whereas control (34) copes well with this task. Because study [11] showed that, in order to stop the rotation of a body by an ion beam, the beam axis should be turned in the same direction as the direction of the body rotation, in the considered case $\beta = \beta_{\min} = 9°$ should be given. Results of integration equation (25) using the control law (34) are shown in Figs. 19 and 20 by dashed lines. The constant control parameter was given as $k = -100$. Since the control $u(\theta')$ is physically bounded above, it was assumed that if $u > 1$, then $u = 1$. Calculations show that the phase trajectory goes into ε-neighborhood of equilibrium position $\theta_k = 891\pi$ in 76,766 s, which is 21 h, 19 minutes, 26 s. The dependence of the control law $u(\theta')$ on an independent variable τ is shown in the Fig. 21.

Control of ion beam axis direction can also be used to space debris detumbling. Results of numerical integration equation (38) using

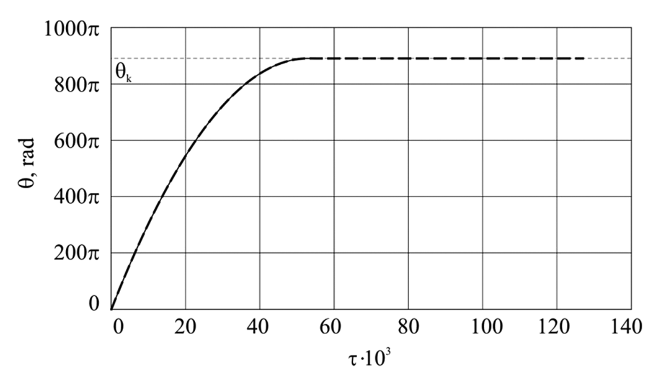

Fig. 19 Space debris detumbling using controls (34) and (43).

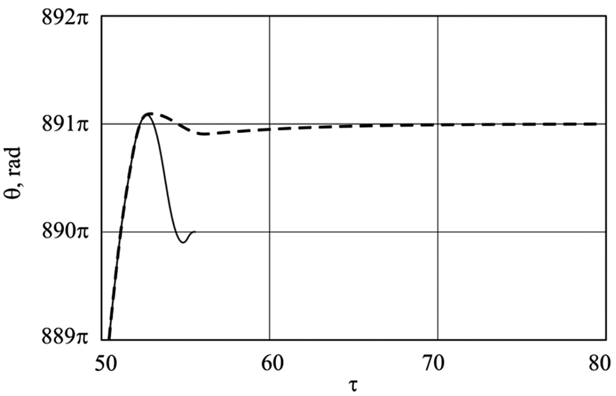

Fig. 20 Final stage of the space debris detumbling using controls (34) and (43).

control law (43) are shown in Figs. 19 and 20 by solid lines. Unlike the case of engine thrust control, stabilization occurs at a different equilibrium position $\theta_k = 890\pi$ (Fig. 20) and takes less time: 33,663 s, which is 9 h, 21 minutes, 3 s.

In both cases, the detumbling process can be divided into two stages. The first stage is the reduction of the angular velocity of the space debris rotation. The second stage is a decrease in the oscillation amplitude. The first stage is the same in both cases. The ion beam axis is deflected by an angle $\beta = \beta_{\min}$ and the ion engine is turned on at full power. This stage ends at the moment $\tau = 52.75$ (Fig. 20), after which control can be carried out in different ways. Calculations showed that the second control method is more preferable from the viewpoint of minimizing stabilization time.

E. Discussion

Analysis of the control laws given by Eqs. (41) and (43) shows that the implementation of the combined control, when simultaneously controlling the ion beam axis deflection angle and the ion engine, is inexpedient because these types of control fundamentally contradict each other. Relay angle control requires the inclusion of thrust at full power, but the thrust control implies varying thrust and even intervals with the engine off. Comparing Figs. 14 and 17 shows that the angle control solves the problem of stabilization for substantially less time compared with the control of the ion engine thrust. The advantage of relay angle control is the possibility of transferring space debris to the equilibrium position for a finite time, whereas engine thrust control allows it to approach this position asymptotically, and it takes infinite time to reach the equilibrium. In addition, the rotation of a light active spacecraft by its orientation engines is considered by the authors to be a simpler task than controlling the engine thrust in a wide range.

It should be noted that the results obtained here are valid for the particular case when the movement occurs in the orbit plane. This ideal case is unrealizable in reality due to the unevenness of the body surface and the presence of external disturbing moments. Therefore, further research is needed to study the effect of out-of-plane motion on the dynamics of controlled space debris motion. It is interesting to try to generalize the proposed control approaches to the case of three-dimensional motion.

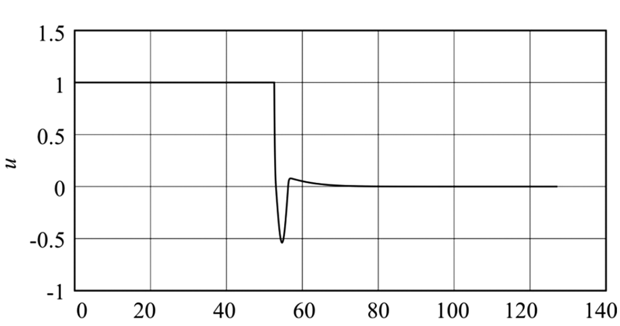

Fig. 21 Control during space debris detumbling by thrust.

Another direction in the development of this work is the stabilization of space debris attitude motion taking into account the influence of the atmosphere. This will allow the use of ion transportation in low Earth orbit. In this study, the case of a circular orbit was considered. Of great practical interest is also the development of the control law of the active spacecraft in an arbitrary orbit, taking into account the relative position of the space debris.

VI. Conclusions

In this paper, the problem of controlling the attitude motion of space debris during its contactless transportation by an ion beam was studied. A mathematical model describing the motion of a mechanical system was constructed. Two ways to control the attitude motion of space debris were considered: by changing the thrust of the ion beam engine and by changing the direction of the ion flux. The control law of the thrust was proposed, ensuring the stabilization of the motion of space debris, and the asymptotic stability of the equilibrium state was proved. It was shown that, in the case of using the second control method, a time-optimal control is relay control. A relay system control law was proposed, allowing it to be transferred to an equilibrium position. The results of numerical simulation proved that controlling the ion flow direction is a more efficient way of stabilizing attitude motion in terms of minimizing the time spent. The proposed laws can be used to stop both oscillations and rotation of space debris. The results of the work can be used in the preparation of space debris cleaning programs on the basis of contactless methods of interaction.

Acknowledgment

This study was supported by the Russian Science Foundation (Project No. 19-19-00085).

References

[1] Shan, M., Guo, J., and Gill, E., “Review and Comparison of Active Space Debris Capturing and Removal Methods,” *Progress in Aerospace Sciences*, Vol. 80, Jan. 2016, pp. 18–32. https://doi.org/10.1016/j.paerosci.2015.11.001

[2] Mark, C. P., and Kamath, S., “Review of Active Space Debris Removal Methods,” *Space Policy*, Vol. 47, Feb. 2019, pp. 194–206. https://doi.org/10.1016/j.spacepol.2018.12.005

[3] Hakima, H., and Emami, M. R., “Assessment of Active Methods for Removal of LEO Debris,” *Acta Astronautica*, Vol. 144, March 2018, pp. 225–243. https://doi.org/10.1016/j.actaastro.2017.12.036

[4] Phipps, C. R., “L’ ADROIT–A Spaceborne Ultraviolet Laser System for Space Debris Clearing,” *Acta Astronautica*, Vol. 104, No. 1, 2014, pp. 243–255. https://doi.org/10.1016/j.actaastro.2014.08.007

[5] Scharring, S., Lorbeer, R. A., and Eckel, H. A., “Heat Accumulation in Laser-Based Removal of Space Debris,” *AIAA Journal*, Vol. 56, No. 6, 2018, pp. 2506–2508. https://doi.org/10.2514/1.J056718

[6] Kumar, R., and Sedwick, R. J., “Despinning Orbital Debris Before Docking Using Laser Ablation,” *Journal of Spacecraft and Rockets*, Vol. 52, No. 4, 2015, pp. 1129–1134. https://doi.org/10.2514/1.A33183

[7] Schaub, H., and Moorer, D. F., “Geosynchronous Large Debris Reorbiter: Challenges and Prospects,” *Journal of the Astronautical Sciences*, Vol. 59, Nos. 1–2, 2014, pp. 161–176. https://doi.org/10.1007/s40295-013-0011-8

[8] Hogan, E., and Schaub, H., “Relative Motion Control for Two-Spacecraft Electrostatic Orbit Corrections,” *Journal of Guidance, Control, and Dynamics*, Vol. 36, No. 1, Jan.–Feb. 2013, pp. 240–249. https://doi.org/10.2514/1.56118

[9] Aslanov, V., and Schaub, H., “Detumbling Attitude Control Analysis Considering an Electrostatic Pusher Configuration,” *Journal of Guidance, Control, and Dynamics*, Vol. 42, No. 4, 2019, pp. 900–909. https://doi.org/10.2514/1.G003966

[10] Bombardelli, C., and Pelaez, J., “Ion Beam Shepherd for Contactless Space Debris Removal,” *Journal of Guidance, Control, and Dynamics*, Vol. 34, No. 3, May–June 2011, pp. 916–920. https://doi.org/10.2514/1.51832

[11] Aslanov, V. S., and Ledkov, A. S., “Attitude Motion of Cylindrical Space Debris During Its Removal by Ion Beam,” *Mathematical Problems in*

Engineering, Vol. 2017, 2017, pp. 1–7. https://doi.org/10.1155/2017/1986374

[12] Urrutxua, H., Bombardelli, C., and Hedo, J. M., "A Preliminary Design Procedure for an Ion-Beam Shepherd Mission," *Aerospace Science and Technology*, Vol. 88, May 2019, pp. 421–435. https://doi.org/10.1016/j.ast.2019.03.038

[13] Merino, M., Ahedo, E., Bombardelli, C., Urrutxua, H., and Peláez, J., "Ion Beam Shepherd Satellite for Space Debris Removal," *Progress in Propulsion Physics*, Vol. 4, March 2013, pp. 789–802. https://doi.org/10.1051/eucass/201304789

[14] Alpatov, A., Cichocki, F., Fokov, A., Khoroshylov, S., Merino, M., and Zakrzhevskii, A., "Determination of the Force Transmitted by an Ion Thruster Plasma Plume to an Orbital Object," *Acta Astronautica*, Vol. 119, Feb.–March 2016, pp. 241–251.
5 https://doi.org/10.1016/j.actaastro.2015.11.020

[15] Nadiradze, A. B., Obukhov, V. A., Pokryshkin, A. I., Popov, G. A., and Svotina, V. V., "Modeling of the Ion Beam Force Impact and Erosive Action on a Large-Sized Object of Technogenic Space Debris," *Proceedings of the Russian Academy of Sciences: Power Engineering*, No. 2, 2016, pp. 146–157.

[16] Cichocki, F., Merino, M., and Ahedo, E., "Spacecraft-Plasma-Debris Interaction in an Ion Beam Shepherd Mission," *Acta Astronautica.*, Vol. 146, May 2018, pp. 216–227. https://doi.org/10.1016/j.actaastro.2018.02.030

[17] Ledkov, A. S., and Aslanov, V. S., "Attitude Motion of Space Debris During Its Removal by Ion Beam Taking Into Account Atmospheric Disturbance," *Journal of Physics: Conference Series*, Vol. 1050, No. 1, 2018, Paper 012041. https://doi.org/10.1088/1742-6596/1050/1/012041

[18] Cichocki, F., Merino, M., Ahedo, E., Smirnova, M., Mingo, A., and Dobkevicius, M., "Electric Propulsion Subsystem Optimization for 'Ion Beam Shepherd' Missions," *Journal of Propulsion and Power*, Vol. 33, No. 2, 2017, pp. 370–378. https://doi.org/10.2514/1.B36105

[19] Alpatov, A., Khoroshylov, S., and Bombardelli, C., "Relative Control of an Ion Beam Shepherd Satellite Using the Impulse Compensation Thruster," *Acta Astronautica*, Vol. 151, Oct. 2018, pp. 543–554. https://doi.org/10.1016/j.actaastro.2018.06.056

[20] Alpatov, A. P., Zakrzhevskii, A. E., Fokov, A. A., and Khoroshylov, S. V., "Determination of Optimal Position of 'Ion Beam Shepherd' with Respect to Space Debris Object," *Technical Mechanics*, No. 2, 2015, pp. 37–48.

[21] Bryson, A. E., and Ho, Y.-C., *Applied Optimal Control: Optimization,
Estimation and Control*, Routledge, New York, 1975, Chap. 4. 6

[22] Merino, M., Ahedo, E., Bombardelli, C., Urrutxua, H., and Pelaez, J., "Hypersonic Plasma Plume Expansion," *32nd International Electric Propulsion Conference*, 2011, pp. 1–14.

[23] Cichocki, F., Merino, M., and Ahedo, E., "Modeling and Simulation of EP Plasma Plume Expansion into Vacuum," *50th AIAA/ASME/SAE/ASEE Joint Propulsion Conference*, 2014, pp. 5008–5024.

[24] Aslanov, V. S., *Rigid Body Dynamics for Space Applications*, Butterworth-Heinemann, Oxford, 2017, Chap. 2.

[25] Hahn, W., *Theory and Application of Liapunov's Direct Method, Computational Methods in Fluid Flow*, Prentice-Hall, Upper Saddle River, NJ, 1963, Chaps. 2, 7.

[26] Panteleev, A. V., and Bortakovskii, A. S., *Teoriya upravleniya v primerakh i zadachakh (Control Theory in the Examples and Problems)*, Visshaya Shkola, Moscow, 2003, Chap. 9.2 (in Russian).

[27] Aslanov, V. S., and Ledkov, A. S., "Dynamics of Towed Large Space Debris Taking into Account Atmospheric Disturbance," *Acta Mechanica*, Vol. 225, No. 9, 2014, pp. 2685–2697. https://doi.org/10.1007/s00707-014-1094-4

[28] Bombardelli, C., Merino, M., Ahedo, E., Peljez, J., Urrutxua, H., Iturri-Torreay, A., and Herrera-Montojoy, J., *Ariadna Call for Ideas: Active Removal of Space Debris Ion Beam Shepherd for Contactless Debris Removal*, 2011, Chap. 2.

[29] Albuja, A. A., Scheeres, D. J., and McMahon, J. W., "Evolution of Angular Velocity for Defunct Satellites as a Result of YORP: An Initial Study," *Advances in Space Research*, Vol. 56, No. 2, 2015, pp. 237–251.
https://doi.org/10.1016/j.asr.2015.04.013 7

[30] Silha, J., Schildknecht, T., Pittet, J. N., Kirchner, G., Steindorfer, M., Kucharski, D., Cerutti-Maori, D., Rosebrock, J., Sommer, S., Leushacke, L., Karrang, P., Kanzler, R., and Krag, H., "Debris Attitude Motion Measurements and Modelling by Combining Different Observation Techniques," *Journal of the British Interplanetary Society*, Vol. 70, 2017, pp. 52–62. https://doi.org/10.7892/boris.106930

Queries

1. AU: Please check that the copyright (©) type is correct. Please note that the code will be added upon publication.
2. AU: LEO has been expanded as low Earth orbit. Please check.
3. AU: "plane motion is a special case of the three-dimensional" is not clear. Please check.
4. AU: LEO has been expanded as low Earth orbit. Please check.
5. AU: Please provide volume number for Refs. [15, 20].
6. AU: Please provide publisher name and location for Refs. [22, 23, 28].
7. AU: Please provide issue number or month of publication for Ref. [30].

Funding Information

The following research funding sources have been associated with your manuscript:

- Russian Science Foundation; Award no. 19-19-00085; Funder ID http://dx.doi.org/10.13039/501100006769

Funding sources listed here can be 1) research grants from outside agencies or organizations or 2) if an author is employed by a U.S. government agency that directly funded this research, this employer also may be listed here as a funding agency. Please confirm that this information is complete and correct for all authors. Edit the Funding Data/Acknowledgments section of your paper if you have changes to funding agency names or grant numbers. Use the funder's full and official name.